IOSR Journal of Agriculture and Veterinary Science (IOSR-JAVS)
e-ISSN: 2319-2380, p-ISSN: 2319-2372. Volume 17, Issue 3 Ser. 1 (March. 2024), PP 01-07
www.iosrjournals.org

Influence Of Superheated Vapor Distribution On Drying Effect Based On Fluent Investigation

Jitan Lian,Guohai Zhang,Jia Yao,Xin Wang,Xipeng Qian,Yihu Wang,
Yuqian Zhao,Qian Dong,Peng Liu,Fukang Zhou
School Of Agricultural Engineering And Food Science,Shandong University Of Technology, Zibo,255000,China

Abstract:
Superheated steam drying technology is a material drying technology with high energy utilization, low environmental pollution, good material treatment effect and high safety with the development of science and technology in recent years. The development of computer digital simulation technology has simplified the testing process in the development of industrial equipment and new technologies. In this paper, the influence of the distribution state of the drying medium in different drying chamber structures on the change rate of the temperature in the drying chamber is compared by using the fluent fluid simulation software, which provides some theoretical basis for the development of superheated steam drying technology.

Key word: *superheated steam drying technology, simulation, drying chamber structure*

Date of Submission: 17-02-2024 Date of Acceptance: 27-02-2024

I. Introduction

Through the superheated steam and materials in contact with the process of moisture, heat exchange, so that the moisture content of the material to reduce the technology is called superheated steam drying technology. Nowadays, superheated steam drying technology is widely used in industrialized production processes such as paper making, sugar making, sludge treatment and wood treatment. Under fixed pressure, saturated steam absorbs heat and turns into unsaturated steam called superheated steam, this unsaturated steam in contact with the material can accommodate the moisture in the material under the action of pressure and temperature, and this process is called superheated steam drying of the material. [1]

Traditional machinery and equipment undergo a series of stages, including design, theoretical validation, prototype construction, prototype testing, and optimization, before officially entering operational use. These stages contribute to an extended research and development (R&D) and production cycle, constrained by environmental and cost considerations. The advent of computer simulation technology has ushered in a new era, leveraging simulation calculation software to replicate partial or complete working conditions of equipment. This innovation significantly truncates the testing phase of equipment manufacturing or optimization, streamlining the overall process [2-4]

In this paper, fluent fluid simulation software is used as a tool to study the distribution state of superheated steam in the drying chamber, and the time required for the temperature change in the drying chamber is taken as the observation to investigate the effect of the change of the drying chamber structure on the drying time.

II. Superheated Steam Drying Principle And Drying Chamber Structure Modelling

Superheated steam drying principle

Superheated steam drying technology constitutes a process wherein superheated steam directly interfaces with the material to extract internal moisture. This method hinges on the principles of heat and mass transfer within the materials. The unsaturated nature of superheated steam allows it to encapsulate moisture in the material, exerting dehumidification and drying effects [5]. The heat and mass transfer dynamics in superheated steam drying involve a reciprocal flow of moisture and heat between the material and the drying medium. External factors influencing the drying efficiency of superheated steam include steam temperature, material moisture content, steam flow rate and direction, and material movement state [6-7].

Structure of superheated steam drying equipment

Superheated steam drying technology is a kind of material drying technology which takes superheated steam as drying medium and carries out heat transfer by convection conduction. Superheated steam is formed by liquid water being heated, phase change occurs, and the resulting water vapor is heated again. The

temperature will exceed the saturated steam temperature at the current pressure. The structure of the superheated steam drying equipment will also be due to the superheated steam itself and the state of the material state of the different changes, such as for drying flakes of superheated steam impingement jet dryer (Deventer et al., 2004); due to the drying of fibrous materials of superheated steam fluidized bed dryer; for drying industrial pulp superheated steam flash dryer(Kiiskinen et al, 1998; Svensson, 1980) and so on. Therefore, the conventional superheated steam drying equipment will include a steam generating device, a steam heating device, a fan, a superheated steam drying tank, a waste heat recovery system, a cyclone separator, a waste liquid collection and treatment system, and the like. In order to simplify the study, the superheated steam drying system can be simplified, Figure 1 is a simplified structural diagram of a superheated steam drying equipment.

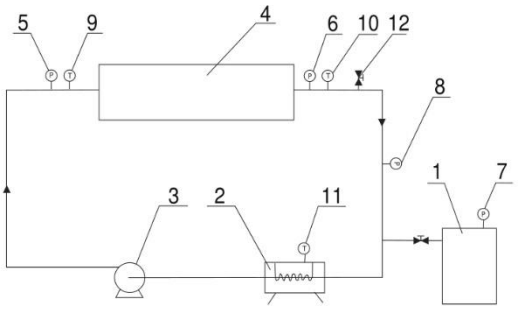

Fig. 1 - Structure of superheated steam drying equipment
1.steam generator; 2.electric heater; 3.centrifugal fan; 4.drying box; 5~8.pressure gauge; 9~11.thermometer; 12.air valve

Influence of material superheated steam drying effect of many factors, this paper for superheated steam in the drying chamber distribution state on the drying effect of the impact of research, explore the square drying chamber structure on the superheated steam flow rate and the impact of the state of motion, so as to speculate on the drying effect of the material in the different state of motion of the superheated steam drying effect of the different.

Modeling of drying chamber structure

In this paper, three drying chamber models are assumed to simulate the effect of superheated vapor distribution state on the heating rate of the drying chamber. The three structures are side inlet, top center outlet; bottom center inlet, top center outlet; bottom center inlet, top center outlet, including the uniform air plate. In order to reduce the calculation time, the model and other conditions are optimized appropriately. The drying chamber model is a rectangle with a side length of 60*60*98mm; the diameter of the air inlet and outlet are both 5mm, and the shape and size of the fluid domain of each model are shown in Fig. 2..

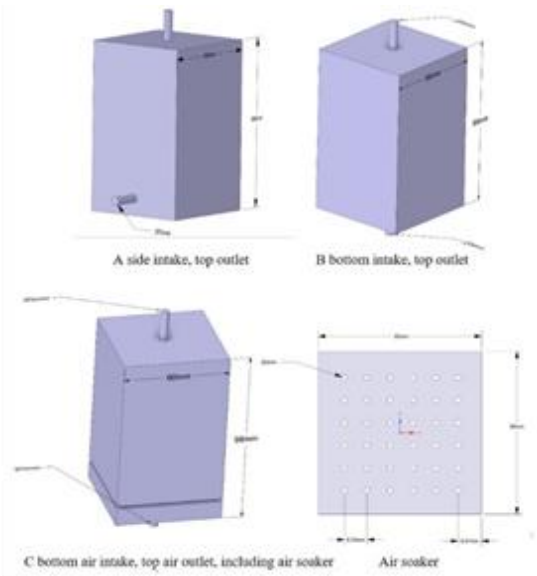

Fig.2. Schematic diagram of the fluid domain of the drying oven model

III. Simulation Condition Setting And Simulation Result Analysis

Simulation Condition Setting

A myriad of external factors influences drying efficiency. This study primarily delves into the impact of the distribution state of the drying medium on the heating effectiveness of the drying chamber. Accordingly, the superheated steam temperature is set at 453.15K, and the inlet flow rate is fixed at 0.8m/s.

Mathematical models

As the most widely used fluid simulation software, Fluent contains many different computational models, such as turbulence model, multiphase flow model, radiation model, discrete phase model, etc. These models can be used to solve different fluid problems on different models.

In this chapter of the model calculation, the basic mathematical equations are included: the mass conservation equation, the momentum conservation equation and the energy conservation equation, and in the simulation, the K-Epsilon turbulence model is applied (Li, 2023), which is the most widely used turbulence model in turbulence simulation, and the equations of the above equations and models are shown in the following table.

Table no 1: Basic governing equations of computational fluid dynamics

Equation for conservation of mass	$\frac{\partial \rho}{\partial t} + \nabla \cdot (\rho \vec{v}) = S_m$
Equation for conservation of momentum	$\frac{\partial}{\partial t}(\rho \vec{v}) + \nabla \cdot \left(\rho \vec{v} \vec{v}\right) = -\nabla p + \nabla \left(\bar{\bar{\tau}}\right) + \rho \vec{g} + \vec{F}$
Equation for conservation of energy	$\frac{\partial}{\partial t}(\rho E) + \nabla \cdot \left(\vec{v}(\rho E + p)\right) = \nabla \cdot \left(k_{eff} \nabla T - \sum_j h_j \vec{J}_j + \left(\bar{\bar{\tau}}_{eff} \cdot \vec{v}\right) \right) + S_h$
k-epsilon	$\frac{\partial}{\partial t}(\rho k) + \frac{\partial}{\partial x_i}(\rho k v_i) = \frac{\partial}{\partial x_j}\left[\left(\mu + \frac{\mu_t}{\sigma_k}\right)\frac{\partial k}{\partial x_j}\right] + G_k + G_b - \rho\varepsilon - Y_m + S_k$
	$\frac{\partial}{\partial t}(\rho \varepsilon) + \frac{\partial}{\partial x_i}(\rho \varepsilon v_i) = \frac{\partial}{\partial x_j}\left[\left(\mu + \frac{\mu_t}{\sigma_\varepsilon}\right)\frac{\partial \varepsilon}{\partial x_j}\right] + C_{1\varepsilon}\frac{\varepsilon}{k}(G_k + C_{3\varepsilon}G_b) - C_{2\varepsilon}\rho\frac{\varepsilon^2}{k} + S_\varepsilon$

Analysis of simulation results

The process of temperature change in the drying chamber is based on the flow of superheated steam as the drying medium in the drying chamber and the exchange of heat between the superheated steam and the air as well as the material in the drying chamber.

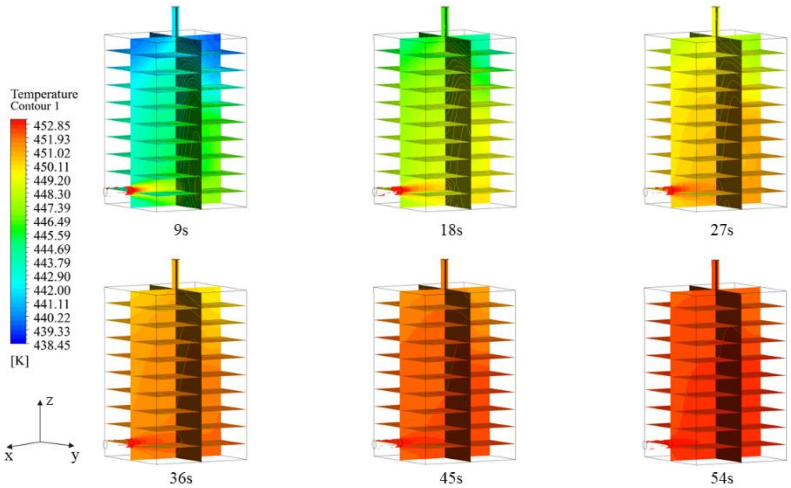

Fig.3. Variation of temperature field in model A

In the A (side inlet, top center outlet) model, after the drying chamber is fed with superheated steam, the temperature inside the drying chamber first starts to rise from the air inlet and the inner wall of the drying chamber opposite to the air inlet, and then heat is exchanged to the rest of the space of the drying chamber. With the increase of time, the temperature difference in the drying chamber will gradually decrease. In the process of heating up the drying chamber, the center of the drying chamber heats up slowly, and the drying rate of the material will be reduced.

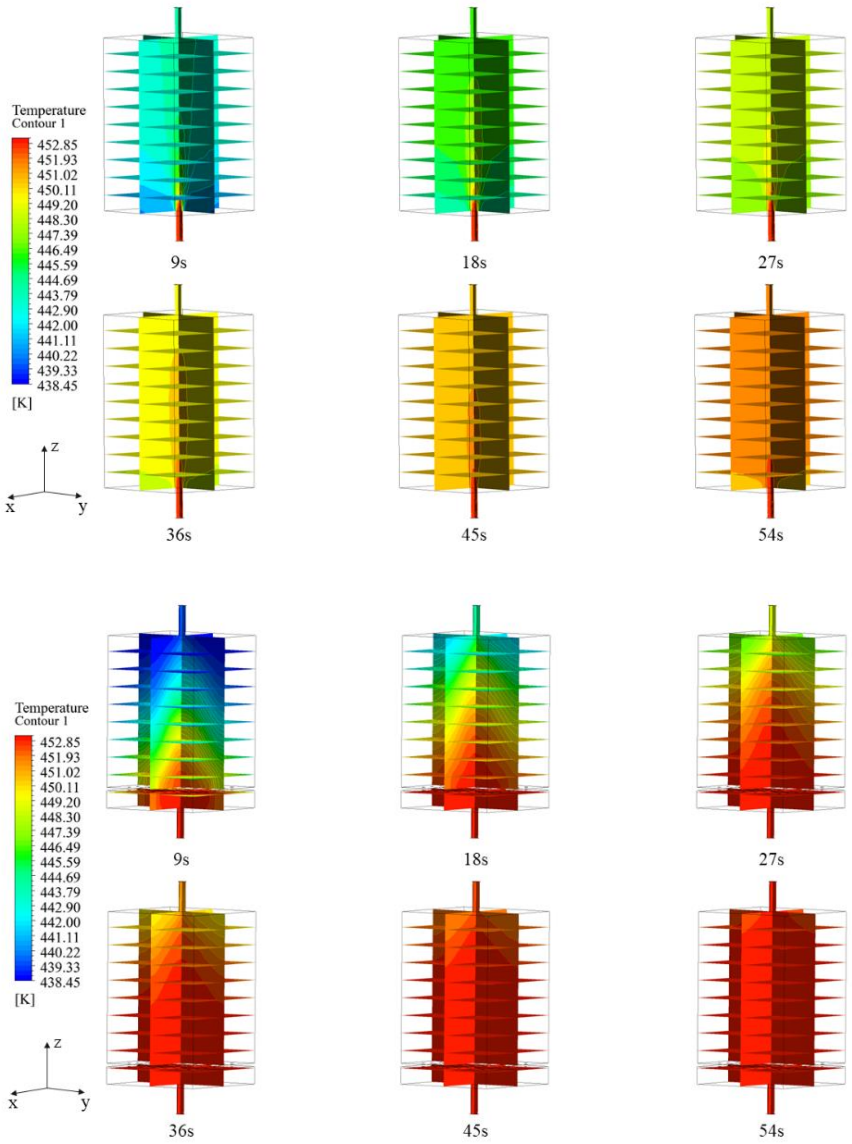

Fig.4. Changes in the temperature field of model B

Model B (bottom center air intake, top center outlet) exhibits a descending temperature trend from the center to the periphery and from the top to the bottom of the chamber. This pattern signifies that heat first reaches the top, then propagates downward, leading to a comparatively slower overall temperature increase. Consequently, the drying efficiency near the bottom or periphery of the chamber is diminished.

Fig.5. Variation of temperature field in C model

In Model C (bottom center inlet, top center outlet, including vapor chamber), superheated steam enters the chamber uniformly under the influence of the vapor chamber. The placement of the vapor chamber alters the steam flow direction, preventing direct escape from the outlet. This modification enhances heat utilization.

Velocity field analysis

While maintaining a constant superheated steam flow rate of 0.8m/s, the varying volume of the air inlet, outlet, and drying chamber impacts gas flow diffusion. Unlike temperature calculations, velocity calculations reach a steady state swiftly. To elucidate results, a narrower range of flow velocities is employed.

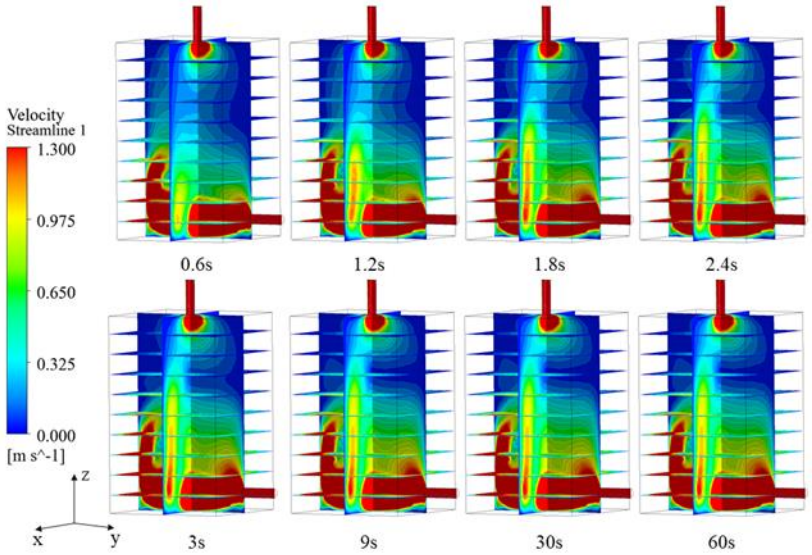

Fig.6. Velocity field change of model A

In the airflow velocity diagram for Model A (side intake, top center outlet), steam velocity surges as it enters the chamber, inducing a chaotic flow field. This chaotic distribution adversely affects material heating uniformity and complicates moisture discharge during the drying process, thereby influencing drying efficiency.

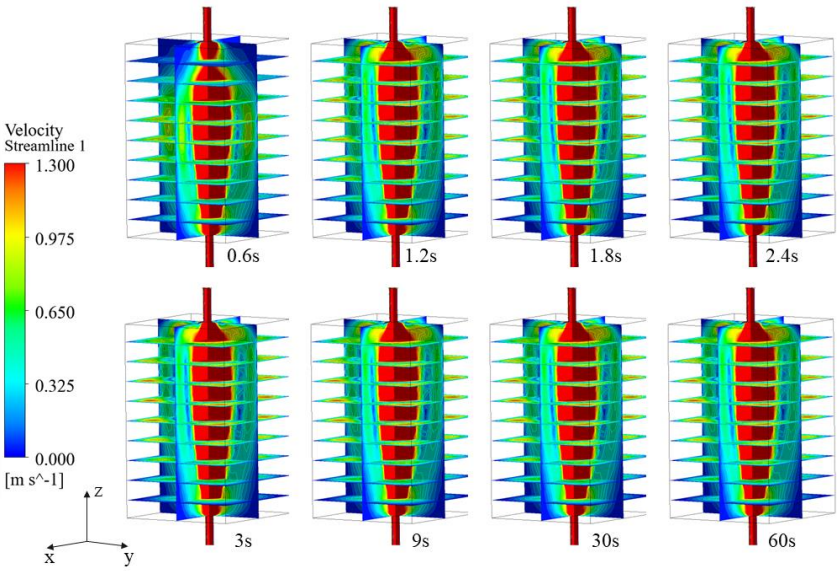

Fig.7. Velocity field change of model B

Model B (bottom center intake, top center outlet) portrays a vertically directed steam flow, resulting in significant differences in flow rates between the chamber center and its periphery. The diffused steam creates a swirl, impeding uniform material drying within the chamber.

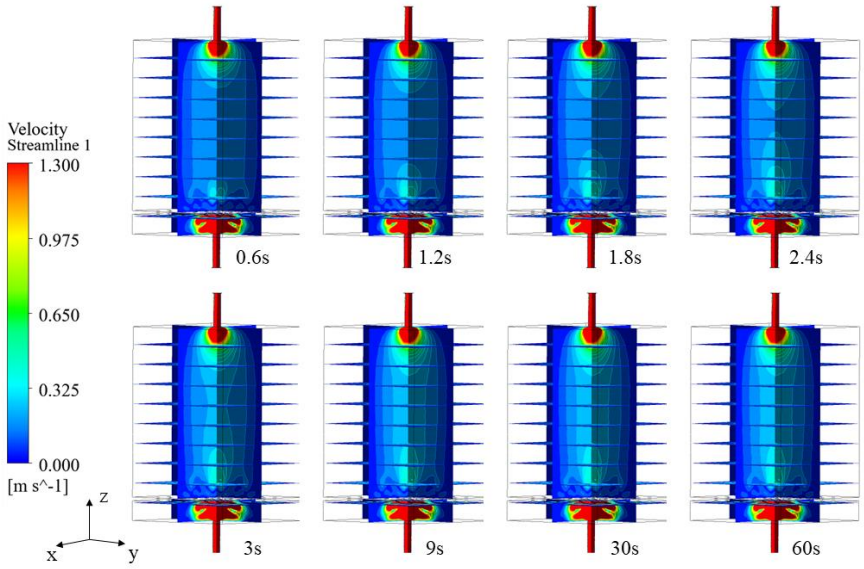

Fig.8. Change of velocity field of C model

Model C (bottom center air intake, top center outlet, including vapor chamber) demonstrates a unique airflow pattern. As superheated steam enters from the air inlet, contact with the vapor chamber induces diffusion. The presence of the vapor chamber minimizes differences in vapor velocity horizontally within the drying chamber.

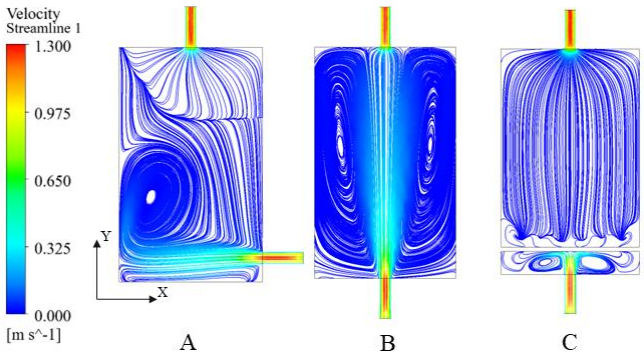

Fig.9. Comparison of the velocity trajectory lines of the three models

Comparing the airflow trajectory lines of Models A, B, and C reveals distinct characteristics. Models A and B exhibit divided trajectory line distributions, resulting in an overall chaotic flow with noticeable swirl phenomena. However, in Model C, the airflow primarily exhibits swirling in a confined space formed by the vapor soaking plate. The airflow in the larger space demonstrates uniform density and a unified direction after partial pressure and diversion by the vapor chamber, reducing the probability and intensity of swirling phenomena.

IV. Conclusion

This study employs Fluent 2021 R1 for numerical simulations of three drying chamber models. A comparative analysis of temperature and velocity field calculations demonstrates that, under equivalent conditions of gas flow velocity and temperature, the flow field distribution profoundly influences the heating effect when heating a container of identical shape and volume. Model C's drying structure, with its vapor chamber-induced division of the drying chamber space and mitigation of gas swirl phenomena, ensures relative stability and uniformity in the majority of the drying chamber. The gradual temperature increase from bottom to top in this model fosters consistent drying conditions, potentially reducing drying times. These findings offer valuable insights into the evolution of subsequent drying technologies and equipment development.

Reference

[1] Deventer H C V, Kosters P S R. Industrial Superheated Steam Drying, Report No. R 2004/239; Tno: Netherlands, 2004.

[2] Hou Xueqing,Ni Lei,Yuan Hao Et Al. Simulation And Analysis Of Temperature Field Of Thermostat Box Based On Fluent[J]. Aut omation And Instrumentation,2023,38(12):10-14.Doi:10.19557/J.Cnki.1001-9944.2023.12.003

[3] Hu, L., Yu, H., Huang, L., Xu, Y., Wu, X. Et Al. (2023). Simulation Research On Coal-Water Slurry Gasification Of Oil-Based Drill Cuttings Based On Fluent. Energy Engineering, 120(9), 1963–1977.

[4] Kiiskinen H,Talja R,Riepen M,Et Al. Single-Sided Steam Impingement Drying Of Paper-Part 1, An Experi-Mental Study [A].In Proceedings Of The 11th Interational Drying Symposium [C].Halkidiki,Greece,1998,19-22

[5] Li Boyang. Numerical Simulation Study Of Nox Generation And Reduction Mechanism In Coke Oven Combustion Chamber[D]. L iaoning University Of Science And Technology,2020.Doi:10.26923/D.Cnki.Gasgc.2020.000163

[6] Liu Yunhong,Li Xiaofang,Miao Shuai Et Al. Ultrasonic-Far Infrared Radiation Drying Characteristics And Microstructure Of Pumpkin Slices[J]. Journal Of Agricultural Engineering,2016,32(10):277-286.

[7] Lu Lin,Zhang Qi,Feng Qing Et Al. Transient Simulation Of Ceramic Billet Drying Based On Porous Medium Model[J]. Journal Of Ceramics,2023,44(04):792-800.Doi:10.13957/J.CnKi.Tcxb.2023.04.021

[8] Li Yan. Research On Mechanism And Parameter Optimization Of Low-Pressure Superheated Steam Drying Of Rice[D].Heilongjiang Bayi Agricultural Reclamation University,2023.Doi:10.27122/D.Cnki.Ghlnu.2023.000006.

[9] Svensson C.Steam Drying Of Pulp [A].In International Drying Symposium [C].Mcgill University,Montreal, August, Hemisphere:N ew York,1980,301-307.

[10] Wang Yongmei,Huang Xiaopeng,Wu Jinfeng. Simulation And Validation Of Flow Field Of Alfalfa Grass Powder Ring Die Granul ator Under Different Process Parameters[J]. Journal Of Agricultural Engineering,2017,33(21):267-274.

[11] Yuan Dongling, Geng Wenguang, Du Rui, Et Al.Superheated Steam Drying Characteristics And Mathematical Model Of Penaeus Vannamei Shrimp[J].Food Science,2020,41(03):62-67.

[12] Zhang Longli. Research On The Effect Of Industrial Waste Composting Treatment And The Change Rule Of Carbonaceous Materi al [D]. China Agricultural University,2014.

[13] Zhang Xukun,Wang Gaomin,Wen Xiangdong Et Al. Shrinkage Characterization Of Superheated Steam And Hot Air Dried Sludge Based On Image Processing[J]. Journal Of Agricultural Engineering,2016,32(19):241-248.